J Electroceram (2006) 16: 151–157
DOI 10.1007/s10832-006-5945-9

Fabrication and structural characterization of interdigitated thin film $La_{1-x}Sr_xCoO_3$(LSCO) electrodes

Anja Bieberle-Hütter · Harry L. Tuller

Received: 29 March 2005 / Revised: 27 October 2005 / Accepted: 31 October 2005

Abstract For the prospective use as micro-Solid Oxide Fuel Cell (μ-SOFC) cathodes and for the investigation of reaction kinetics, $La_{1-x}Sr_xCoO_3$ (LSCO) mixed ionic electronic conducting thin films were deposited by DC and RF sputtering onto a number of different substrate materials and characterized. Standard photolithographic and wet chemical etching methods were utilized to *microstructure* the LSCO films and XRD, SEM, AFM, WDS, and RBS were used to characterize their structure, topography, and chemistry. Sputtering resulted in very homogeneous and smooth thin crystalline films with Sr deficiency and submicron sized grains. Hydrochloric acid was found to readily etch LSCO with the etching quality strongly dependent on substrate material. LSCO films were most easily etched when deposited directly on silicon substrates, etched at intermediate rates when deposited on Gd:CeO_2 films, and most resistant to etching after deposition onto single crystal yttria stabilized zirconia (YSZ) substrates. Imperfect etching was attributed to interface formation and the presence of impurities.

Keywords Lanthanum strontium cobaltate (LSCO) · Sputtering · Thin film · Microfabrication · Micro-SOFC

A. Bieberle-Hütter (✉) · H. L. Tuller
Crystal Physics & Electroceramics Laboratory,
Department of Materials Science and Engineering,
Massachusetts Institute of Technology, Cambridge,
MA 02139 USA
e-mail: anja.bieberle@alumni.ethz.ch

Present address:
Nonmetallic Inorganic Materials, Department of Materials Science,
Swiss Federal Institute of Technology, ETH Zürich, Zürich, Switzerland

1. Introduction

The rapid growth in portable electronic devices has stimulated interest in the development of compatible miniaturized high energy density power sources. In one approach, Si wafers are being considered as a platform for micro-Solid Oxide Fuel Cells (μ-SOFC) [1] and thus thin film deposition techniques, such as sputtering and pulsed laser deposition, take on special importance. Thin films not only allow for the reduction of the operating temperature (~900°C in traditional SOFC systems), but also allow considerable miniaturization of the entire system down to chip size dimensions. In addition, thin films are ideal vehicles for studying reaction mechanisms, since well-defined geometries can be fabricated allowing for a more systematic investigation of system kinetics. Since the cathode side of traditional SOFC systems is considered to be a major source of loss, more detailed investigations of the key candidate materials and the mechanisms limiting reaction kinetics are warranted [2].

Lanthanum strontium cobalt oxide (LSCO) was selected as a prospective cathode material for μ-SOFC given its attractiveness as a mixed ionic electronic conductor and its high activity for oxygen reduction [3]. It is usually applied as a thick film in SOFC applications. Few reports exist on thin film deposition of ceramic SOFC materials. In particular, suitable deposition techniques for prospective industrial use, the deposition of multilayer structures, and the chemical and electrical interaction with adjacent thin films and substrates have not been investigated in detail.

Pulsed Laser Deposition, PLD, a method allowing excellent stoichiometric reproducibility between target and thin film, has been previously used to study LSCO thin film deposition [4–7]. The investigation of sputtered LSCO films has been largely restricted to the field of ferroelectrics where they find use as electrically conducting contacts under ambient

conditions [8]. Sputtering is a well accepted and standardized method in industry for large scale applications and could be an attractive method for fabrication of low cost μ-SOFC. Recently, Ringuede and Fouletier examined the performance of sputtered LSCO films on YSZ pellets [9] and Klenov et al. investigated the relationship between film microstructure and electrical resistivity [10]. In most studies, LSCO films have been deposited onto MgO, $SrTiO_3$, and $LaAlO_3$ single crystals. Only recently have YSZ single crystal substrates been used. No studies on the *microstructuring* of LSCO films by lithographic means are known to the best of the authors' knowledge.

In this paper, the deposition and structural characterization of sputtered LSCO thin films, integrated onto prospective SOFC electrolyte materials, such as YSZ and CGO, and suitable substrate materials are discussed. The special focus of the paper is related to the lithographic *microstructuring* of LSCO thin films. In another paper, we focus on the electrical and electrochemical characterization of the microstructured electrodes [11].

Table 1 (a) DC and (b) RF sputtering parameters for LSCO

(a)		
Parameter	Value	Unit
Substrate temperature	500	°C
Power	25	W
Base pressure	$\sim 3 \cdot 10^{-7}$	Torr
Working pressure	20	mTorr
Gas composition Ar:O_2	97:3	–
Deposition rate	47	nm/h

(b)		
Parameter	Value	Unit
Substrate temperature	500	°C
Power	50	W
Base pressure	$\sim 3 \cdot 10^{-7}$	Torr
Working pressure	10	mTorr
Gas composition Ar:O_2	9:1	–
Deposition rate	33	nm/h

2. Experimental procedure

Two inch diameter $La_{1-x}Sr_xCoO_3$ ($x = 0.5$) sputtering targets were fabricated from the following starting powders: La_2O_3 (99.99%, Alfa Aesar), $SrCO_3$ (99%, Alfa Aesar), $CoCO_3$ (99%, Alfa Aesar). The powders were weighed in the correct proportion and were then ball-milled in distilled water with a mix of 5 mm and 10 mm diameter zirconia spheres for 24 h. The slurry was dried on a hotplate and ground by mortar. The powder was then calcined at 1150°C for 5 h in air (heating and cooling rate = 5°C/min). After calcination, the powder was ground with a mortar and ball-milled for another 24 h in 2 weight % polyvinyl alcohol. After drying the slurry on a hotplate, the powder was ground thoroughly and sieved using 100 mesh sieve (wire diameter = 114 μm, opening 140 μm). The target was then pressed in a uniaxial press at about 62 MPa and sintered at 1250°C for 5 h in an oxygen atmosphere (heating and cooling rate = 1°C/min). The lateral shrinkage of the target during sintering was about 15%. Finally, the planar targets were bonded to copper backing plates using Ag paste and heat treatment at ~200°C for 30 min.

Sputtering of LSCO was carried out in a Kurt J. Lesker sputtering system with deposition parameters for the DC and RF sputtering processes listed in Table 1. The thin films were deposited onto a number of different substrates including: (1) a SiO_2wafer coated with $Ce_{0.84}Gd_{0.16}O_{2-\delta}$ thin film (CGO; by RF sputtering, $P = 45$ W, $p = 20$ mTorr, Ar:O_2 = 97:3, T = 500°C, thickness = 204 nm), (2) a Si wafer coated with 1 μm Si_xN_y (grown using a Vertical Thermal Reactor CVD process) and a sputtered layer of CGO (thickness ~500 nm), and (3) YSZ single crystals with and without a sputtered CGO intermediate layer (thickness ~350 nm). The substrates were rotated during deposition in order to guarantee a homogeneous film thickness.

The LSCO thin films were *microstructured* by standard photolithography and wet chemical etching: First, the substrates were annealed for about 10 min at 130°C to remove adsorbed water molecules. A thin film of Hexamethyldisilizane (HMDS) was applied at a spinning rate of 400 RPM as adhesion promoter for the photoresist. The HMDS was applied three times and the substrates were then annealed at 130°C for about 10 min. Afterwards, the positive photoresist OCG 825-20-CS (distributed by Hubbard Hall, Waterbury, CT, USA) was spun for 6 s at 750 RPM, followed by 30 s at 2000 RPM resulting in a photoresist thickness of about 1 μm. The substrate was pre-baked at 90°C for 30 min and then exposed under UV light (365 nm, 4 mW) for 4 s using a glass photolithography mask with the pattern structure. The photoresist was developed in OCG 934 1:1 (distributed by Hubbard Hall, Waterbury, CT, USA) for about 1 min and rinsed with deionized water. Finally, the substrate was post-baked at 130°C for 40 min. After the photolithography process, the substrates were etched in dilute hydrochloric acid (HCl, 36.5–38%, product number: 2062-04, Mallinckrodt Chemicals, Phillipsburg, NJ, USA) which was further diluted with water typically in the ratio 1:15 = HCl : water. Etching was stopped when no residue of LSCO was detected in the etched areas under the light microscope (maximum magnification 100×).

The patterns were shaped as interdigitated electrodes (IDE) with equidistant fingers, f, and spacing, s, between 15 μm and 100 μm. This corresponded to triple phase boundary lengths, l_{tpb}, of 171.9 cm to 25.3 cm and a constant electrode

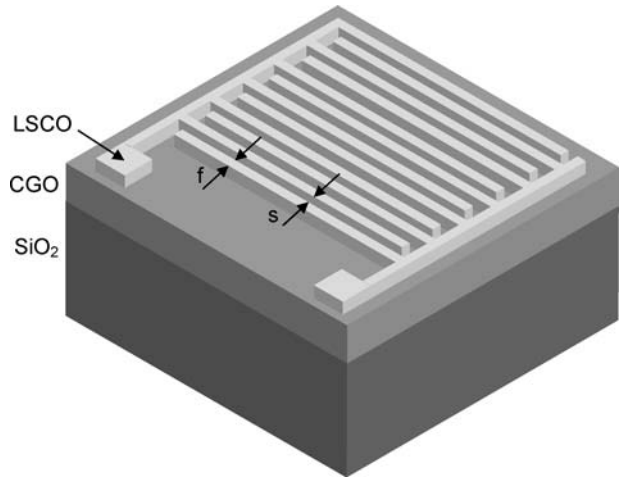

Fig. 1 Sketch of an interdigitated LSCO electrode on top of a CGO thin film integrated onto a SiO_2 wafer: f = finger and s = spacing

area of ∼0.25 cm^2. A sketch of a typical pattern geometry and layer structure is shown in Fig. 1.

The thin films were characterized by scanning electron microscopy SEM (FEI/Philips XL30 FEG ESEM and Leo Gemini 1530 FESEM), wavelength dispersive spectroscopy WDS (Jeol JXA-733), Rutherford backscattering spectroscopy RBS (Tandetron, General Ionex), and surface profilometry (Tencor P-10). Powder X-ray diffraction (XRD) was carried out with a Rigaku 185 nm Bragg Brettano Diffractometer with 18 kW rotating anode and was analyzed using the JADE 6 program form Materials Data, Inc. (MDI). A glancing angle attachment was used in case of thin film analysis. A D8 XRD diffractometer from Bruker was used for the characterization of the target.

3. Results and discussion

3.1. Thin film characterization

Sputtering resulted in very homogeneous and smooth thin films with submicron sized grains. A SEM top view image of a LSCO thin film shows a grain size of 20–30 nm with a very low surface roughness (Fig. 2(a)). No significant difference between the RF and the DC deposited films was found with respect to the surface topography. However, DC sputtered films were more susceptible to cracking than RF sputtered films. All films were completely dense and well adherent to the substrate. They grew homogeneously without a columnar structure (Fig. 2(b)). SEM analysis gave no evidence for any interface reaction or phase formation at the interface.

The LSCO thin films were single phase, crystalline, and without preferred orientation as confirmed by XRD analysis. The rather broad peaks indicate a very small crystallite size. Table 2 contains a detailed analysis of the XRD data of the powder, the target, and the thin film, respectively. The

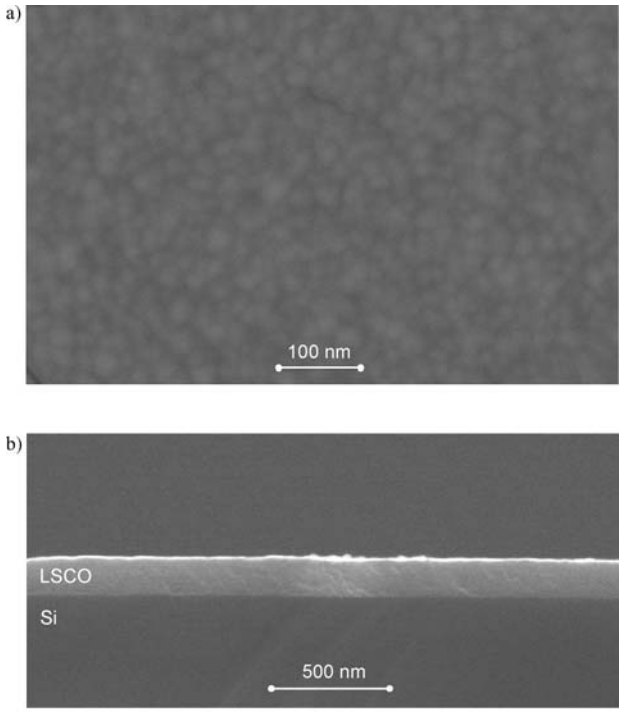

Fig. 2 SEM images (a) top view, (b) cross section of a sputtered LSCO thin film on Si: grain size = 20−30 nm, film thickness = 166 nm (for sputtering conditions refer to Table 1(a))

reference data from the PDF cards as well as CGO thin film data were added for comparison. Relative intensities, I, are given for each data set with decreasing number for decreasing intensity. Very similar peak intensities and peak positions were found for the LSCO, $x = 0.5$ (LSCO 0.5), reference, the powder, and the target data. The reference data reports peak splitting for most of the LSCO peaks. However, since the 2θ difference between split peaks is very small ($< 0.2^\circ$) and the peaks of the measured data are very broad due to the small grain size, it is not possible to resolve the splitting for the powder and the target data. Due to the broad peaks, it is also not possible to unambiguously verify the exact stoichiometry of the prepared materials by this method. Compounds of lower strontium content result only in a small shift in peak positions which cannot be resolved in the observed spectra. WDS and RBS were later used to verify the stoichiometry of the deposited thin films.

Small additional XRD peaks, detected in the powder and the target data (not listed in Table 2), are attributed to Ba impurities contained in the starting $SrCO_3$ powder. They were not detected in the thin film due to the detection limit. An analysis of the entire system, i.e. LSCO–CGO–SiO_2, was not possible, given that LSCO and CGO peaks overlap at most 2θ angles. It was verified, however, that CGO thin films on SiO_2 have the same peak positions as the reference data for CGO ($x = 0.2$).

The stoichiometries of the deposited layers were analyzed by Wavelength Dispersive Spectroscopy (WDS) and

Table 2 XRD peak positions (two theta) and relative intensities, *I*, of reference data (LSCO and CGO) and of LSCO powder, target, and thin film

LSCO 0.5 PDF# 048-0122	*I*	CGO 0.2 PDF# 050-0201	*I*	LSCO 0.5 powder	*I*	LSCO 0.5 target	*I*	LSCO 0.5 on Si	*I*	LSCO 0.5 on CGO-SiO_2	*I*	CGO on SiO_2	*I*
23.18	7			23.4	7	23	7	23.5	1	23.3	5		
		28.531	2							28.6	2	28.5	1
32.979	1												
33.057	1	33.056	1	33.1	1	32.9	1	32	3	33	1	33.2	7
38.86	10			38.4	8	NA		38.2	7	NA			
40.688	4			40.7	4	40.5	4	NA		NA			
40.815	4												
47.384	2	47.426	4	47.5	2	47.6	2	47.7	4	47.4	6	47.4	3
53.311	8												
53.426	8			53.5	9	53.2	8	52.6	6	NA			
		56.256	3							56.3	3	56.2	2
58.859	3												
58.933	3	58.966	7	59	3	58.9	3	58.6	2	58.5	8	59	5
59.095	3												
69.132	5												
69.348	5	69.301	5	69.5	5	69.3	5	69.2	5	69.4	7	NA	
74.01	9												
74.105	9												
74.302	9			74.3	10	74.3	9	NA		NA			
		76.576	8							NA		76.5	6
78.814	6												
78.938	6	78.937	6	79.1	6	79.1	6	78.7	8	79	4	79	4

Note: The lower the number in column *I* the higher the intensity of the XRD peak.

Rutherford Backscattering Spectroscopy (RBS). Both WDS and RBS indicate very similar results with a strong deviation from the expected stoichiometry. Instead of the nominal target composition $La_{0.5}Sr_{0.5}CoO_3$, the stoichiometry of the thin film was $La_{0.84}Sr_{0.16}Co_{0.67}O_x$ (WDS data; assumption: La + Sr = 1). Thus, sputtering results in Co and Sr deficient layers. The Sr deficiency could be avoided in the future by co-sputtering simultaneously from a LSCO and a Sr or Sr-oxide target. The exact Sr content has then to be calibrated by adjusting the sputtering power. The exact oxygen stoichiometry cannot be well determined with either method.

The in-plane conductivity, σ, of the LSCO thin films was measured on MgO substrates: σ was about 300 S/cm at 300°C and about 700 S/cm at 600°C. These values are very close to LSCO bulk data reported by Mineshige et al. [12] and Tokura et al. [13] measured on samples with similar Sr deficiencies. More detailed discussion on the electrical properties of the LSCO films is given in [11].

3.2. Fabrication of interdigitated electrodes

3.2.1. Selection of etchant

All interdigitated electrodes in this study were etched in dilute hydrochloric acid (HCl) which readily etched the LSCO. Nitric acid [14] and phosphoric acid [7] are mentioned in the literature for etching large LSCO contact pads. However, in this study, etching with nitric compared to hydrochloric acid was found to be less successful due to concerns about photoresist stability. Reactive ion etching with SF6 was ineffective in attacking LSCO thin films.

HCl was considered to be a suitable etchant for the system under investigation given that all electrolyte and substrate materials were expected to be resistant to HCl. Nevertheless, in order to verify electrolyte and substrate inertness, deposited CGO films were carefully tested with respect to possible HCl attack. Microstructural degradation, in particular etching of the grain boundaries, was investigated by AFM. CGO thin films deposited onto Si-based substrates were exposed, for up to 5 min, to dilute HCl. No difference in the Rms (∼10–12 nm) between as-deposited and etched samples was found. In addition, possible degradation of an as-deposited Pt electroded CGO thin film and an identical sample following exposure to HCl was studied by electrochemical impedance spectroscopy (EIS). The EIS data was collected as described in [11, 15]. No significant differences in the electrochemical response between the two measurements were found (Fig. 3). Hence, it is concluded that HCl does not attack CGO thin films, while readily etching LSCO.

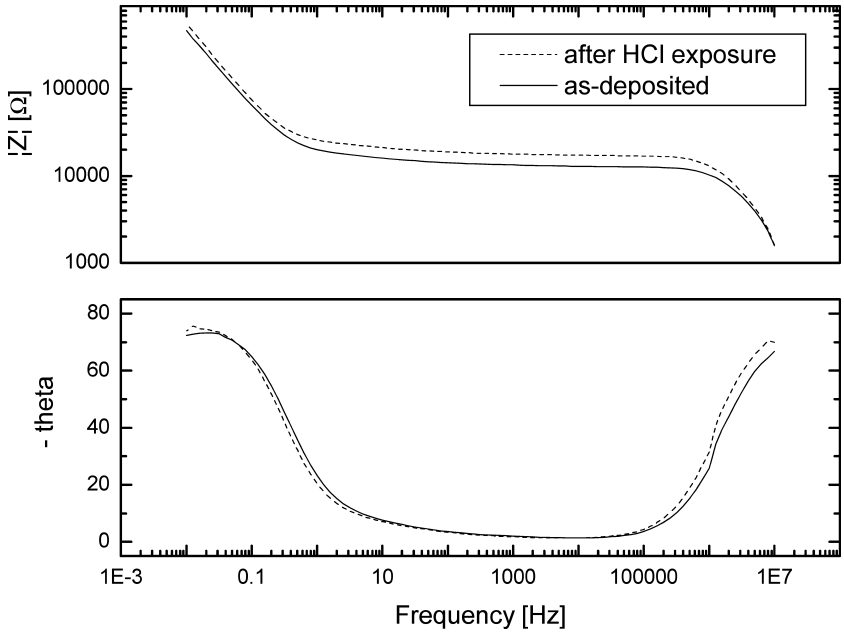

Fig. 3 Electrochemical impedance spectroscopy data, magnitude of impedance and phase angle vs. frequency, of an as-deposited Pt/CGO/SiO_2 test sample compared to an identical sample after HCl exposure

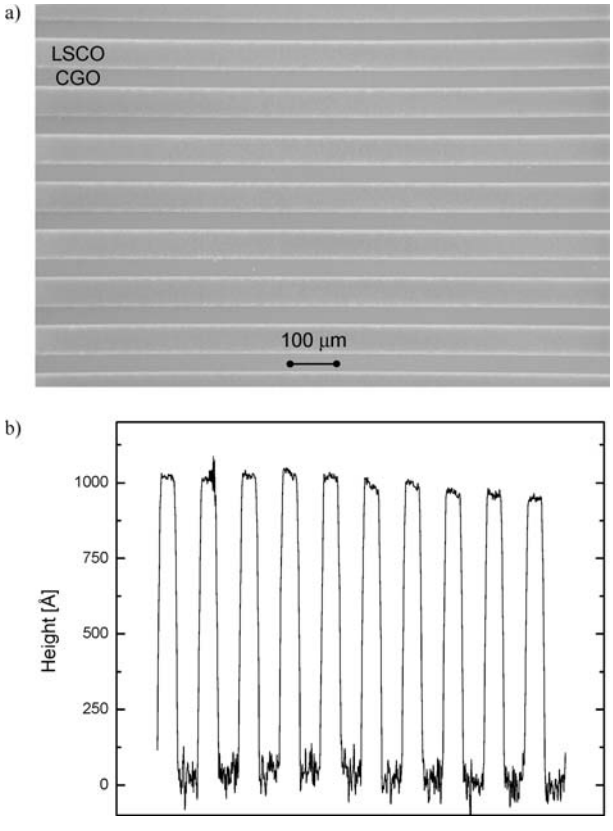

Fig. 4 (a) SEM top view image and (b) surface profile of a microstructured LSCO thin film on CGO−SiO_2 (f = LSCO stripe = 50 μm, s = CGO stripe = 50 μm)

3.2.2. Etch quality and influence of substrate material

A typical LSCO thin film following etching is shown in Fig. 4: continuous stripes of LSCO on CGO are observed (Fig. 4(a)). No LSCO residue is visible in the spacing between the electrodes, i.e. on the CGO surface. The surface profile indicates that the CGO surface is rougher than the LSCO thin film. The etched edges of the pattern are very sharp (Fig. 5(b)).

A higher magnification view of the etched edges of the electrodes shows irregularities and greater porosity as compared to the dense inner section of the electrode stripes (Fig. 5). This is believed to be due to a thinning of the photoresist at the edges of the photoresist pattern during the etch process leaving the underlying LSCO thin film susceptible to attack (Fig. 5(a)). For cracked films, the etch solution seeps into the cracks through capillary forces resulting in a widening of the cracks at the edge (Fig. 5(b)). The CGO thin film deposited at 300˚C did not crack during LSCO deposition at 500˚C (Fig. 6). The rougher surface topography of the CGO compared to the LSCO surface is clearly visible in Fig. 6.

The substrate material was found to have considerable influence on the etch results as well. LSCO thin films deposited onto blank Si wafers, where the native oxide layer was not removed prior to LSCO deposition, were readily etched without leaving any residue in the spaces between the electrodes. The surface profile indicates very sharp edges. In contrast, the quality of LSCO micropatterns is less satisfactory on most common SOFC materials, such as YSZ and CGO. The major part of the LSCO film is easily etched at a rate similar to LSCO films deposited onto blank Si. However, close to the LSCO-substrate interface, the etch rate decreases. Finally, some residue sometimes remains in the form of islands in the spacing between the electrodes which cannot be removed even following extended etch times or use of concentrated acid solutions (Fig. 7). Fortunately, only few non-interconnected islands are left after etching. Hence,

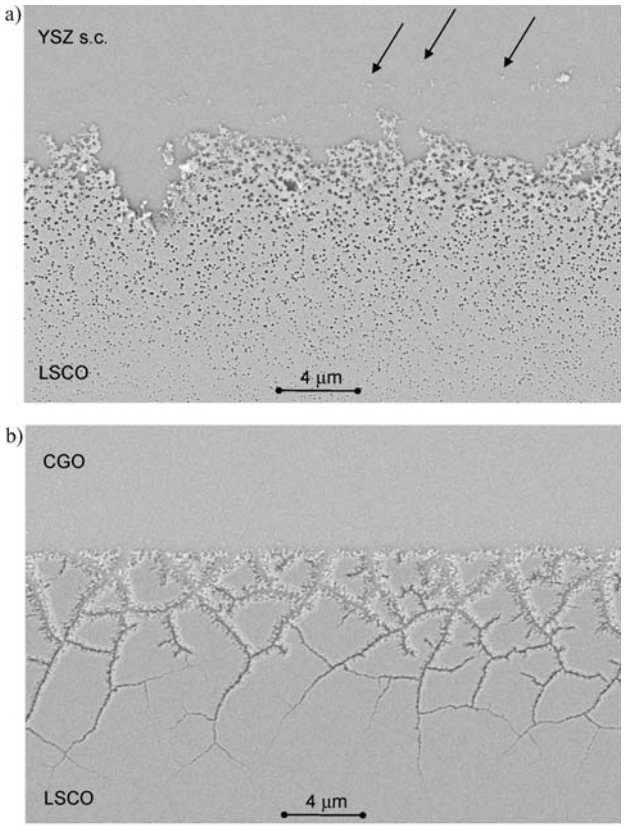

Fig. 5 SEM top view images of etch edges of *microstructured* LSCO thin films: (a) crack-free LSCO thin film on YSZ s.c. (arrows indicate examples of etch resistant residue), (b) cracked LSCO thin film on CGO–SiO_2

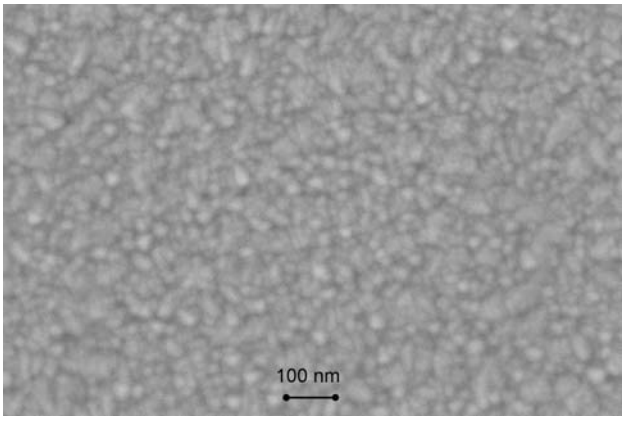

Fig. 6 SEM top view image of CGO thin film in the spacing of two fingers after etching of LSCO (LSCO on CGO–SiO_2)

the electrode conductance is little affected by the residue. Decreased etch rates between LSCO-substrate interface and incomplete etching is most evident with YSZ single crystals (Fig. 5(a) and Fig. 7) and therefore does not allow for the fabrication of LSCO pattern with feature sizes below 100 μm on YSZ single crystals. This is much less pronounced with CGO or YSZ thin films.

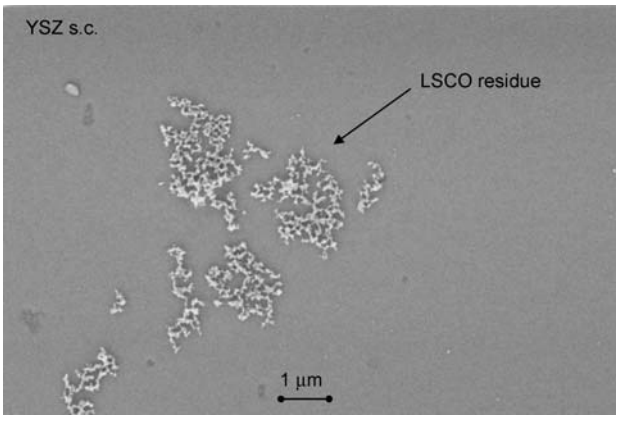

Fig. 7 SEM top view image of etch resistant LSCO island in the spacing of two fingers (LSCO on YSZ s.c.)

The source of the acid resistant residue may be either due to interdiffusion, interface reactions or impurities. To date, interface reaction products, such as the formation of $La_2Zr_2O_7$, while reported at much higher temperatures, have not been reported at as low temperatures as used in the deposition of the thin films in this study [16]. It is, however, possible that the highly energetic sputtering process locally heats the interface and thereby facilitates the formation of a second phase. XRD, XPS, and RBS analyses did not reveal any interface formation or modifications in the thin films or the substrate which might be related to new phase formation. Due to limited resolution of these techniques, TEM analysis is planned for further investigation in the near future.

On the other hand, impurities can originate from the substrate and might segregate to the interface between the freshly deposited thin film and the substrate during high temperature deposition. A mixed or glassy phase, resistant to HCl etching, could be formed. Since thin films normally have fewer impurities than bulk material, this could also explain why etching of LSCO films deposited on a thin film, such as CGO, is more effective than on YSZ single crystals.

4. Summary and conclusions

LSCO thin films were successfully deposited by RF and DC sputtering onto different prospective substrate materials for μ-SOFC application. The layers were smooth, dense, well adherent, crystalline, single phase and with submicron-sized grains. The stoichiometry of the thin films was found to be Sr deficient. Depending on the sputtering process, some cracks could be detected in the films. HCl was found to serve as an appropriate etchant for *microstructuring* of LSCO. While it readily etches LSCO, it does not attack adjacent materials, such as CGO thin films.

The quality of the etching was found to depend on the substrate material. While HCl readily etches LSCO deposited

onto Si, the etch time becomes longer for LSCO deposited onto CGO thin films. LSCO films on YSZ single crystal substrates require long etch times and exhibit unsatisfactory etch quality likely due to an interface reaction between LSCO and YSZ.

The lithographic process described in this work was found to serve well as a means for *microstructuring* LSCO electrodes both for kinetic studies and for μ-SOFC applications. Since kinetic studies do not necessarily require very small feature sizes, the discussed method can be directly used for the fabrication of well-defined geometries with sharp edges, not possible using shadow masks during the deposition process. For use in fabricating μ-SOFC, the utility of this approach will depend on the anticipated feature size of the LSCO *microstructure*. For very small feature sizes (<50 μm), the observed interface reactions with certain substrates, e.g. YSZ, must first be resolved. Further, factors relating to purity of the substrates or whether the highly energetic deposition process needs to be modified must also be addressed. PLD, characterized by improved stoichiometry control and possibly less intense substrate interactions, may be an alternative attractive deposition method. One must, however, take into account its inability to cover large surface areas as uniformly as sputtering.

Acknowledgments This work was supported by the DOD Multidisciplinary University Research Initiative (MURI) program administered by the Army Research Office under Grant DAAD 19-01-1-0566. A. B.-H. gratefully acknowledges fellowship support from the Swiss National Foundation Grant PBEZ2-102368 and the Deutsche Forschungsgemeinschaft Grant BI 826/1-1. The authors gratefully acknowledge assistance with conductivity measurements by Martin Søgaard, Risø National Laboratory, Denmark, use of the high resolution SEM (Jeol Gemini 1530) at the Institute of Nonmetallic Inorganic Materials, ETH Zurich, and the many stimulating discussions with Joshua Hertz, Il-Doo Kim and Kurt Broderick of MIT.

References

1. C.D. Baertsch, K.F. Jensen, J.L. Hertz, H.L. Tuller, S.T. Vengallatore, S.M. Spearing, and M.A. Schmidt, *J. Mat. Res.*, **19**, 2604 (2004).
2. J.M. Ralph, C. Rossignol, and R. Kumar, *J. Electrochem. Soc.,* **150**, A1518 (2003).
3. J.M. Ralph, A.C. Schoeler, and M. Kumpelt, *J. Mat. Sci.,* **36**, 1161 (2001).
4. X. Chen, N. Wu, A. Ignatiev, Z. Zhang, and W.-K. Chu, *Thin Solid Films,* **350,** 130 (1999).
5. X. Chen, S. Wang, Y.L. Yang, L. Smith, N.J. Wu, B.-I. Kim, S.S. Perry, A.J. Jacobson, and A. Ignatiev, *Solid State Ionics,* **146**, 405 (2002).
6. S. Stemmer, A.J. Jacobson, X. Chen, and A. Ignatiev, *J. Appl. Phys.,* **90**, 3319 (2001).
7. Q.X. Jia, P.N. Arendt, C. Kwon, J.M. Roper, Y. Fan, J.R. Groves, and S.R. Foltyn, *J. Vac. Sci. Technol. A,* **16**, 1380 (1998).
8. I.-D. Kim, W.-Y. Choi, G.-P. Choi, J.-H. Park, C.H. Lee, and H.-G. Kim, *J. Kor. Phys. Soc.,* **35,** S496 (1999).
9. A. Ringuede and J. Fouletier, *Solid State Ionics,* **139**, 167 (2001).
10. D.O. Klenov, W. Donner, L. Chen, A.J. Jacobson, and S. Stemmer, *J. Mater. Res.,* **18**, 188 (2003).
11. A. Bieberle-Hütter, M. Søgaard, and H.L. Tuller, *Solid State Ionics* (2005) submitted.
12. A. Mineshige, M. Inaba, T. Yao, Z. Ogumi, K. Kikuchi, and M. Kawase, *J. Solid State Chem.,* **121**, 423 (1996).
13. Y. Tokura, Y. Okimoto, S. Yamaguchi, H. Taniguchi, T. Kimura, and H. Takagi, *Phys. Rev. B*, **58**, R1699 (1998).
14. J. Lee, R. Ramesh, and V.G. Keramidas, *Mat. Res. Soc. Symp. Proc.,* **361,** 67 (1995).
15. J.L. Hertz and H.L. Tuller, *J. Electroceramics*, **13**, 663 (2004).
16. H. Yokokawa and T. Horita, in *High Temperature Solid Oxide Fuel Cells —Fundamentals, Design and Application*, edited by S.C. Singhal and K. Kendall (Elsevier, Oxford, 2003), p. 119.